This article is published as part of a themed issue of **Photochemical & Photobiological Sciences** containing a collection of papers from the

5th European Meeting on Solar Chemistry and Photocatalysis: Environmental Application

Edited by Vincenzo Augugliaro, Leonardo Palmisano and Sixto Malato

Published in **issue 5, 2009**

Low-temperature synthesis and characterization of TiO$_2$ and TiO$_2$–ZrO$_2$ photocatalytically active thin films†

Ksenija Maver,[a] Urška Lavrenčič Štangar,*[a] Urh Černigoj,[a] Silvia Gross[b] and Romana Cerc Korošec[c]

Transparent TiO$_2$ and TiO$_2$–ZrO$_2$ (molar ratio Zr/Ti = 0.1) thin films were produced by low-temperature sol–gel processing from nanocrystalline aqueous based solutions. The structural features and compositions of the films treated at room temperature, 100 °C and 500 °C were investigated by X-ray diffraction, X-ray photoelectron spectroscopy and thermal analysis. Addition of zirconia increased specific surface area (140–230 m^2 g^{-1}) and hindered the growth of anatase crystallites, exhibiting a constant size of 6–7 nm in the whole temperature range. These significant changes with respect to pure TiO$_2$ in anatase crystalline form did not result in significantly and systematically different photocatalytic activity, which was evaluated in terms of aqueous pollutant degradation (azo-dye in water) and self-cleaning ability (fatty contaminant deposit). The films treated at only 100 °C showed excellent photocatalytic activity towards azo-dye degradation. Contact angle measurements of aged and contaminated surfaces revealed a fast or sharp hydrophilicity gain under UVA illumination. Accordingly, the results of this study confirmed the potential application of advantageous low-temperature films in water treatment as well as for self-cleaning surfaces.

Introduction

Despite the enormous number of scientific publications related to photocatalysis in recent decades, there are obviously still some problems to be solved towards wider applications of photocatalytic materials. One of the important issues is certainly to make a material with the highest efficiency/price ratio. The requirements for the material depend on its final use, being in the field of water treatment, air purification, deodorization, antimicrobial and self-cleaning surfaces.[1] In the sense of covering a broad area of applications, the development of highly efficient and transparent coatings through an easy and reproducible preparation procedure is desirable.

The sol–gel technique has emerged as one of the promising techniques for growing TiO$_2$ thin films at ambient conditions. Conventionally, the desired nanocrystallinity and photocatalytic activity are achieved with surfactant-assisted sol–gel processing.[2] This method requires relatively high calcination temperatures (500 °C) to remove the surfactant and to induce the formation of the anatase crystalline phase. These high processing temperatures, however, represent a major obstacle to many applications. Another approach is to overcome high crystallization temperature and to promote crystallization as early as during the formation of the sol.[3]

TiO$_2$ in its anatase crystalline modification is generally accepted as the most efficient photocatalyst,[1] but for instance also brookite films were found to be highly active in a gas–solid photoreactor.[4] Further improvements of activity or abrasion resistance of a sol–gel titania film were attempted by introducing a second component such as silica,[5] which may substantially modify its performance even at low concentrations. It has already been shown that the addition of zirconia increases the final surface area of the catalyst,[6–12] the anatase-to-rutile transition temperature,[7–9] the surface acidity and the overall adsorption and hydrophilic properties.[8–12] All of these changes are considered positive for enhancement of the photocatalytic activity. On the other hand, ZrO$_2$ has a bandgap much larger (~5 eV)[8,10] than TiO$_2$ (3.0–3.2 eV)[1] and, therefore, cannot act as a photocatalyst under UVA illumination. This and the fact that it perturbs the titania network crystallinity presumably have adverse effect on the photocatalytic activity even at lower zirconia content.

This work describes the low-temperature sol–gel preparation of transparent TiO$_2$ and TiO$_2$–ZrO$_2$ thin films, in view of examining the role of zirconia at given preparation conditions in: (i) thermal development of the anatase phase, (ii) the surface and in-depth composition of the films, (iii) the modification of the surface area, (iv) the natural and photoinduced hydrophilicity of the films, and (v) the photocatalytic activity of the films towards azo-dye and fatty deposit degradation.

Experimental

Thin film preparation by low-temperature sol–gel processing

A primary titania sol was prepared from titanium(IV) isopropoxide (Ti(O^{i}Pr)$_4$) precursor by following the idea of low-temperature

[a] Laboratory for Environmental Research, University of Nova Gorica, Vipavska 13, 5001, Nova Gorica, Slovenia. E-mail: urska.lavrencic@p-ng.si; Fax: +386 5 3315 296; Tel: +386 5 3315 241
[b] CNR-ISTM, Dipartimento di Scienze Chimiche, Università degli Studi di Padova, and INSTM, via Marzolo 1, 35131, Padova, Italy
[c] Faculty of Chemistry and Chemical Technology, University of Ljubljana, Aškerčeva cesta 5, 1000, Ljubljana, Slovenia. E-mail: romana.cerc-korosec@fkkt.uni-lj.si; Fax: +386 1 2419 220; Tel: +386 1 2419 136

preparation route proposed by Yun *et al.*[3] A mixture of 28.8 g of Ti(O^{i}Pr)$_4$ (Acros Organics) and 4.0 g of absolute ethanol (Riedel-de Haen) was added during vigorous stirring into a solution of 2.8 g of conc. HNO$_3$ (Acros Organics) in 180 g of deionized water. The resulting sol was refluxed at 85 °C for 48 h. The milky white sol was stable, without significant sedimentation, at room temperature for several months.

TiO$_2$–ZrO$_2$ sol was prepared by adding both corresponding alkoxides simultaneously at the beginning of the sol preparation process. A mixture of 25.9 g of Ti(O^{i}Pr)$_4$, 3.5 g of zirconium butoxide (Zr(OBu)$_4$, tetrabutyl zirconate solution, 80 wt% in 1-butanol) (Aldrich) (Ti : Zr = 10 : 1) and 4.0 g of absolute ethanol was poured during vigorous stirring added into a solution of 2.8 g of conc. HNO$_3$ in 180 g of deionized water. The resulting sol was refluxed at 85 °C for 48 h. The translucent sol was very stable, without any sedimentation, at room temperature for several months.

Transparent titania and titania–zirconia films were deposited on both sides of soda-lime glass slides (25 × 70 mm), on silicon wafers (19 × 19 mm) and on microscope cover glasses (22 × 22 mm) by a dip-coating method. The substrates were cleaned with ethanol and/or distilled water and dried before film deposition. They were then dipped into the sol at room temperature and withdrawn at the speed of 10 cm min^{-1}. The substrates coated with gel films were left to dry at room temperature and then heated predominantly at 100 °C and 500 °C. The coating-heating cycles were performed up to three times to obtain thicker films.

Materials characterization

The thicknesses of some representative films were measured by a Taylor-Hobson Talysurf profilometer and determined to fall in the range between 130 and 180 nm for one coating–heating cycle. UV-Vis spectra of the films and dye solutions were recorded on a Hewlett-Packard 8453 UV-Vis spectrophotometer. XRD measurements of thin films, deposited on silicon resins, were obtained using a PANalytical X'Pert PRO diffractometer with Cu Kα (λ = 0.1542 nm) radiation from 20 to 60 2θ in steps of 0.034 and a time per step of 500 s. Thermogravimetric analysis (TG) of thin film samples, deposited on microscope cover glasses, was performed on a Perkin Elmer TGA7 Instrument. It should be emphasized that X-ray diffraction as well as thermal analysis were performed also on thin film samples and not only on their powder counterparts as is usually done to avoid the more demanding procedure of thin film analysis. The BET specific surface area of powder samples was determined by measuring the nitrogen adsorption–desorption isotherms at 77 K, using Micromeritics-ASAP 2020 chemisorption system.

The surface and in-depth composition of the thin films were analyzed by XPS on a Perkin-Elmer Φ5600ci spectrometer using standard Al Kα (1486.6 eV) radiation working at 350 W. The working pressure was <5 × 10^{-8} Pa. The spectrometer was calibrated by assuming the binding energy (BE) of the Au4f$_{7/2}$ line at 83.9 eV with respect to the Fermi level. The standard deviation for the BE values was 0.15 eV. Survey scans (187.85 pass energy, 1 eV per step, 25 ms per step) were obtained in the 0–1300 eV range. Detailed scans (58.7 eV pass energy, 0.1 eV per step, 25 ms per step) were recorded for the O1s, C1s, Ti2p, TiKLL, Zr3d, Zr3p, Ti3p, Ti3s regions. Depth profiles were carried out by Ar$^+$ sputtering at

3 keV with an argon partial pressure of 5 × 10^{-6} Pa. A specimen area of 2 × 2 mm was sputtered. Samples were introduced directly, by a fast entry lock system, into the XPS analytical chamber. The assignments of the peaks were carried out by using the values reported in appropriate databases.[13]

The hydrophilic and hydrophobic surface characteristics of the thin films were evaluated by examining the contact angle between the thin film and a water droplet. Deionized water droplets (pH = 5.7) of 0.5 μL volume were spread onto the films surface using a microsyringe. The water contact angles were measured at ambient temperature, using a CAM 100 FireWire horizontal video camera module with a protractor eyepiece. For this purpose, the Contact Angle Meter (CAM 100), KSV Instrument, Ltd. Finland, was used.

Photocatalytic activity measurements

The photocatalytic activity of sol–gel derived titania and titania–zirconia thin films was tested by measuring the photodegradation of (i) Plasmocorinth B as a model azo-dye pollutant in water, and (ii) methyl stearate as a model fatty contaminant for determining the self-cleaning ability of the films.

To evaluate the photocatalytic activity *in situ* at the solid–liquid interface, a batch-type continuous flow reactor with on-line connection to the UV-Vis spectrophotometer was used.[14] The photocatalytic cell was filled with 6 mL of Plasmocorinth B aqueous solution (the dye concentration was 40 mg L^{-1}), continuously purged with oxygen during normal irradiation and cooled by tap water. A solution of NaBr and Pb(NO$_3$)$_2$ in water was used as a 335 nm cut-off filter in front of the photocatalytic cell and a 125 W Xe lamp (Cermax xenon parabolic lamp) as a light source. A thin film deposited on a soda-lime glass slide was immersed in the dye solution next to the wall of the photocatalytic cell and irradiated (surface 23 × 23 mm) along the normal direction. The absorbance of the azo-dye solution during UVA irradiation was on-line measured and the intensity of the characteristic peak at λ = 526 nm as a function of irradiation time was plotted (*i.e.* at the wavelength where Plasmocorinth B showed maximum absorption).

To evaluate the photocatalytic activity at the solid–solid interface,[15] the films were pre-irradiated for 120 min to induce super-hydrophilicity (irradiance source was a 40 W UV lamp, wavelengths in the range 310–390 nm, peak at 355 nm). The photon irradiance in the sample compartment was estimated by potassium ferrioxalate actinometry and determined to be 8.67 × 10^{-9} einstein cm^{-2} s^{-1} (≈4 mW cm^{-2}). The solution of methyl stearate (0.1 M) in n-hexane was used for the films contamination. Thin layer of methyl stearate was deposited by dip-coating technique with a pulling speed of 10 cm min^{-1}. By measuring the water contact angle before and during the UV irradiation of the films the photocatalytic activity was followed.

Results and discussion

Optical properties

All the thin films obtained in this work were crack-free and transparent over the whole visible spectral range (not shown here). As observed in our previous studies,[14] an increase in the number

of dippings produced a red-shift in the absorption edge of the film. The shift has been ascribed to differences in the size of the crystallites. Thicker films that underwent longer heat treatment by repeated coating–heating cycles have relatively larger anatase crystallites and this causes the onset of absorption to shift to the longer wavelengths.[16] Accordingly, also higher heat-treatment temperature (500 °C compared to 100 °C) resulted in a slight red-shift, corresponding to stronger ultraviolet absorption. A red-shift of the absorption edge also indicates a decrease in the band gap with increasing number of coating–heating cycles and heat-treatment temperature.

Structural and compositional properties

First, a low-temperature formation of a functional anatase phase was checked by XRD. From XRD patterns of the films (Fig. 1) it is evident that crystalline anatase phase was present already at a room temperature in both types of samples and was retained during isothermal treatment for 3 h at 500 °C. For as-deposited TiO_2 film the average crystallite size was around 5 nm, calculated from the width of anatase (101) reflection by using the Scherrer equation. During heat-treatment at 500 °C, the crystallites grew larger to 12 nm. In the film having TiO_2–ZrO_2 composition, crystallites were slightly larger at room temperature (6 nm) and they remained nearly of the same size after thermal treatment at 500 °C (7 nm). This is in accordance with the BET specific surface areas, which were higher for TiO_2–ZrO_2 composites (226 m^2 g^{-1} and 148 m^2 g^{-1} for thermal treatment at 100 °C and 500 °C, resp.) than for TiO_2 (208 m^2 g^{-1} at 100 °C and 51 m^2 g^{-1} at 500 °C). It has already been reported that a small addition of ZrO_2 inhibits the formation of well-crystalline particles of TiO_2.[10] In spite of simultaneous hydrolysis of Ti and Zr alkoxides during the preparation of our samples, no significant shift of (101) anatase peak was observed and therefore the formation of a solid solution $Ti_{1-x}Zr_xO_2$ cannot be confirmed.[7] On the other hand, no crystalline ZrO_2 phase was detected in diffractograms up to 500 °C, thus suggesting that ZrO_2 remains either amorphous or in the form of very small particles and hinders the growth of anatase crystallites.[7,11]
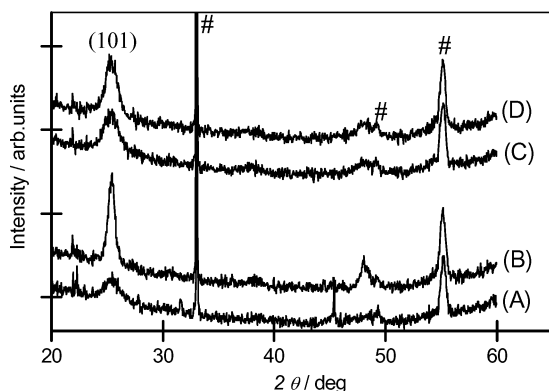

Fig. 1 X-Ray diffraction patterns of thin film samples, deposited on silicon resins: (A) TiO_2 at room temperature, (B) TiO_2 exposed for 3 h to 500 °C, (C) TiO_2–ZrO_2 at room temperature, (D) TiO_2–ZrO_2 exposed for 3 h to 500 °C. # denotes the reflection of a substrate.

The surface and in-depth composition of the mixed titania–zirconia sample (TiO_2–ZrO_2 at 500 °C) as well as the chemical state and environment of the involved species were thoroughly analyzed by XPS. Depth profiles were carried out by controlled removal (sputtering) of the surface of the sample, addressed by bombardment with Ar^+ ions, followed by analysis, as described in the experimental part. All the involved species (O, C, Zr, Ti) can be clearly seen in Fig. 2a, reporting the survey spectrum of the sample after 5 min of sputtering.
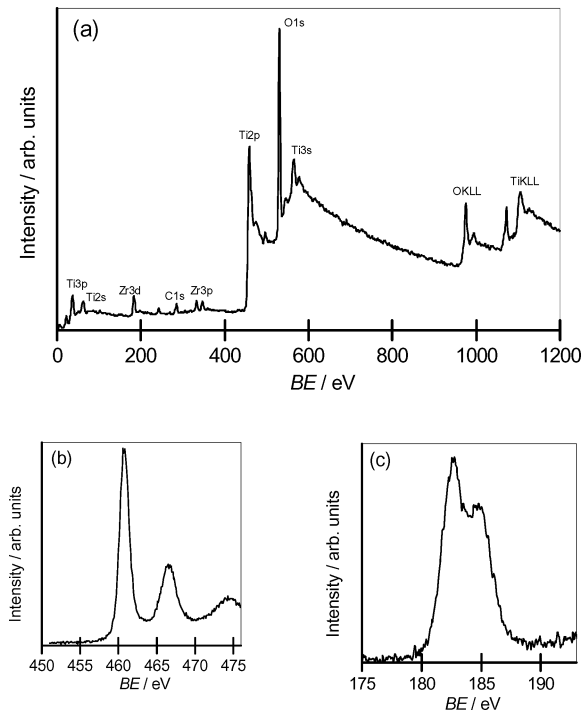

Fig. 2 Survey spectrum of TiO_2–ZrO_2 film (heat-treated at 500 °C) after 5′ sputtering (a), Ti2p region (b) and Zr3d region (c) of the same sample on the surface. The peaks in Fig. (b) and (c) are *not* corrected for charging effects.

As far as the surface and in-depth composition of the samples is concerned, the atomic percentages of the different chemical species as a function of the sputtering time are reported in Table 1. It evidences that the Ti/Zr atomic ratio is constant through the whole sputtered layer and very close to the expected nominal value (*i.e.* 10). This finding demonstrates a good compositional homogeneity of the prepared sample and an even distribution of the guest zirconium species in the host titania matrix.

On the surface of the sample a high carbon content (32%) was detected. This can be ascribed to the surface adsorption of organic contaminants from the air and is also reflected in an increased water contact angle by ageing (see below). Its amount remarkably decreased upon sputtering, but carbon is still present

Table 1 In-depth atomic composition of TiO_2–ZrO_2 film (heat treated at 500 °C) obtained by XPS measurements at different sputtering times (min)

Min	%C	%O	%Ti	%Zr	Ti/Zr
0	32.2	50.1	16.3	1.4	11.5
5	21.9	54.0	22.1	1.9	11.6
10	14.6	57.7	25.4	2.2	11.5
20	17.8	54.1	25.9	2.3	11.4
60	14.2	67.2	16.9	1.6	10.6

in considerable amount (*ca.* 15%, Table 1). The reason is most probably the penetration of organic contaminants further into the film's structure. From the TG curve of the film (Fig. 3) it is evident that thermal decomposition is completed already before 400 °C, meaning that a high carbon content could not be attributed to thermally undecomposed organic precursors. After 60 min of sputtering, Zr, Ti and O are still well detectable in the survey spectrum (data not shown), but also an Si signal could be observed, thus indicating that the interface with the underlying soda-lime substrate was reached.
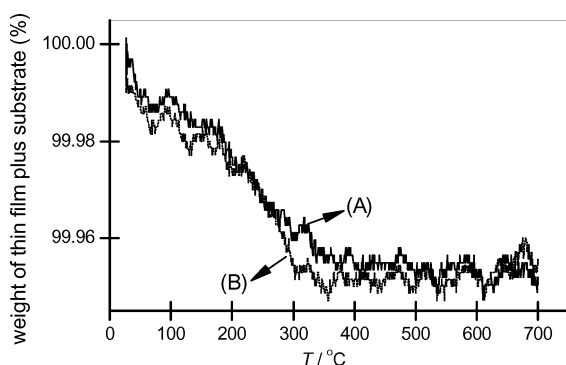

Fig. 3 Thermogravimetric curve of (A) TiO$_2$ thin film and (B) TiO$_2$–ZrO$_2$ thin film, both deposited on a miscroscope cover glass. The initial weight of a thin film and a substrate was around 50 mg.

Looking at the chemical state and environment of titanium, the BE of the Ti$2p$ peak ranges between 457.6 and 458.4 eV (Fig. 2b). These values are slightly lower than those reported for Ti$2p$ in TiO$_2$ (458.5–459.2 eV). Upon sputtering, a significant broadening of the Ti$2p$ region was observed. This can be ascribed to (i) a partial reduction of Ti(IV) to Ti(III) due to the preferential sputtering of oxygen and ion bombardment induced damage,[17] and (ii) to the formation of understoichiometric TiO$_x$ species.

Concerning zirconium, the BE values for the Zr$3d$ and Zr$3p$ regions range from 182.4 to 183.5 eV and from 332.6 to 333.2 eV, respectively. These values are very close to the values reported for pure zirconia (182.3–183.0 eV and 332.5 eV, respectively).[13] The literature data for the mixed system SiO$_2$–ZrO$_2$ in the same molar ratio (*i.e.* Si : Zr = 10 : 1) show a remarkable shift at higher values of the Zr$3d$ BE.[18] In this case the shift exceeded the expected values of about 1.0–1.5 eV. In this system, the zirconia particles are dispersed in a silica matrix. Zirconium experiences a chemical environment that is substantially different from that in bulk zirconia. In fact, silicon is more electronegative than zirconium and the Si–O–Si bonds around Zr are expected to withdraw more electron density than the Zr–O environment in the case of a pure zirconium oxide (or Ti–O environment in the case of TiO$_2$–ZrO$_2$ system). This implies a shift of the Zr$3d$ BE towards higher BEs.

To get a better insight in the chemical environment of the zirconium atom and to ascertain whether further components occur due to the presence of the Ti–O network, the Zr$3d$ peak region was deconvoluted. The Zr$3d$ region shown in Fig. 2c, which could be deconvoluted with two components, is ascribed to the Zr$3d_{3/2}$ and Zr$3d_{5/2}$ peaks. On this basis and on the basis of XRD results, the presence of Zr–O–Ti mixed bonds could not be evidenced, although the first treatment of EXAFS results (work

still in progress) showed the existence of Zr–O–Ti bonds in the TiO$_2$–ZrO$_2$ sample heat-treated at 500 °C.

Thermogravimetric analysis of thin films deposited on a substrate is a demanding technique, since the weight loss is in the range of buoyancy and aerodynamic effect.[19] In Fig. 3 the TG curves of both films, deposited on microscope cover glass, are presented. They are not smooth due to very small weight change and therefore we cannot clearly distinguish at which temperature the removal of adsorbed water was completed and other processes begin, but most probably this is around 100 °C. Results obtained from evolved gas analysis of the corresponding xerogel samples (data not shown here), where the gases released during TG measurement were analysed with a mass spectrometer, show that further weight loss up to 400 °C is associated with removal of decomposition products of unhydrolysed isopropoxy groups, nitrates and water molecules. Water is evolved during a condensation reaction[20] and due to dihydroxylation process of the surface as well. Both TG curves are almost identical, indicating a similar degree of surface hydroxylation on both types of films. On the contrary, we observed that titania–silica films (using the same titania sol) exhibited a much bigger mass loss associated with a highly hydroxylated surface.

Photocatalytic activity studies by *in situ* UV-Vis spectroscopy

Photocatalytic activity of the films towards the degradation of azo dye Plasmocorinth B in the aqueous phase was measured. Fig. 4 shows photobleaching curves–absorbance at 526 nm as a function of irradiation time of the dye solution in contact with various thin films and in comparison with a photocatalytic standard (Degussa P25 powder immobilized on a glass slide[21]).
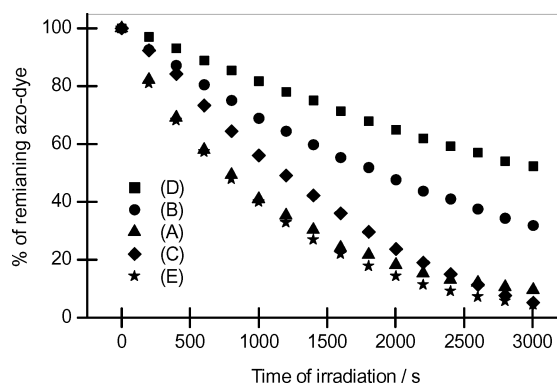

Fig. 4 Photocatalytic degradation of azo dye Plasmocorinth B in contact with various thin films: (A) TiO$_2$ heat-treated at 100 °C, (B) TiO$_2$ at 500 °C, (C) TiO$_2$–ZrO$_2$ at 100 °C, (D) TiO$_2$–ZrO$_2$ at 500 °C, and (E) standard Degussa P25 powder immobilized on a glass slide.

The films prepared at low temperatures showed very good photocatalytic efficiency toward azo-dye degradation, comparable with the efficiency of the Degussa sample in this solid–liquid system (Fig. 4). The photodegradation rates were high even if the films were deposited by only two coating cycles. They became much lower when those films were heat treated at 500 °C, which is the opposite behaviour to films made from alcoholic sols.[14] These studies can be compared because the same photoreactor set-up and other experimental conditions were used. Here, the presence of an anatase phase already at room temperature is responsible

for this opposite behaviour and high activity without calcination. The crystallinity and UV absorption are further enhanced with the heating, but other factors contributing to detrimental effect of calcination obviously prevailed. These can be: migration of sodium ions from the substrates into the film by heating (confirmed also in our previous study[2]), surface area and film roughness decrease, or higher recombination due to some other reasons. However, the results are characteristic for this experimental set-up and cannot be generalized.

At our experimental conditions, we could not confirm the beneficial influence of zirconia addition on the photocatalytic activity of the films (Fig. 4). Although TiO_2–ZrO_2 samples had up to 40% more film mass than TiO_2 (determined by weighing of the substrates before and after film deposition), a homogeneous distribution of zirconia (as shown by XPS profiles) and near to optimum zirconia concentration,[7] they showed worse photocatalytic properties. This does not agree with many reports in the literature claiming the positive effect of zirconia addition, though it was mainly found for suspended catalysts.[6,8,10,12] We confirmed that higher surface area and smaller particles in case of TiO_2–ZrO_2 do not correlate with a photoactivity rise,[7] probably because the lower degree of crystallinity and higher number of crystalline defects favor recombination rate of holes and electrons.

Photocatalytic activity studies by contact angle measurements

The situation is somewhat different when studying the photoactivity at solid–solid interface by water contact angle measurements of a surface contaminated with a methyl stearate layer. First, the water contact angles were measured on the freshly prepared titania and titania–zirconia thin films deposited on glass substrates. The initial values were in the range from 11° to 15° for TiO_2 and from 6° to 11° for TiO_2–ZrO_2. After 3 days of ageing these values increased due to air contamination (18–31° for TiO_2 and 15–20° for TiO_2–ZrO_2). The lower value in the range corresponds to thermally treated films at 500 °C, characterized by more complete removal of organic components and impurities from the film surface. We could systematically observe a slightly higher degree of natural hydrophilicity of the mixed oxide system, which is ascribed to increased surface acidity of zirconia-modified titania.[8,10]

The ten-days aged films were then exposed to UVA radiation for up to 150 min (Fig. 5a). The results clearly show the photoinduced superhydrophilic nature of both types of films. The kinetics of contact angle decrease was slightly slower with TiO_2 film treated at 100 °C than with the others, but then already at 60 min it dropped to the lowest value. The Pilkington Activ™ self-cleaning glass was measured as a reference. A fast drop of contact angle to its superhydrophilic value was not expected with this commercial glass because it has a much thinner and very compact titania film. Then, these "clean" hydrophilic surfaces were contaminated with a methyl stearate layer and the corresponding contact angles abruptly increased to a hydrophobic value of around 100°. The decrease of the hydrophobicity was followed as a function of UV irradiation time (Fig. 5b). All the investigated films acted as photocatalysts, enabling a gradual degradation of the methyl stearate with an aid of UV irradiation, also at the solid–solid interface. Corresponding measurements of IR spectra of the films deposited on silicon wafers (data not shown here) were done to be sure of the methyl stearate photodegradation process. Surprisingly, the TiO_2 film treated at 100 °C markedly deviated from the other three, which showed similar effectiveness. A much slower response of the former sample (which on the other hand demonstrated the best performance towards azo-dye degradation in water) may be ascribed to some undefined effects that caused a "poisoning" or altering of the surface and retarded the beginning of methyl stearate degradation, which then proceeded with a sudden decrease of a contact angle to its lowest value. The reasons remain unclear and would need further investigations. It seems that specific surface area was high enough in all cases ($> 50 \, m^2 \, g^{-1}$ in powder analogues), so it was not the rate determining factor. The results somehow correlate with the XRD patterns of the four films (Fig. 1) in the respect that the highly developed anatase phase with the crystallite sizes of 12 nm (TiO_2 at 500 °C) favors the photodegradation rate over the least developed crystalline structure (TiO_2 at 100 °C). The both TiO_2–ZrO_2 films showed similar XRD patterns and also similar (fast) degradation kinetics (Fig. 5b), but of course there are many other parameters than crystallinity that influence the photocatalytic behaviour. In this particular photocatalytic test, an advantage of zirconia addition was evident only for low heat-treatment temperatures of the films.

Conclusion

The modification of titania with zirconia has been found to influence the specific surface area, anatase crystallite sizes and natural
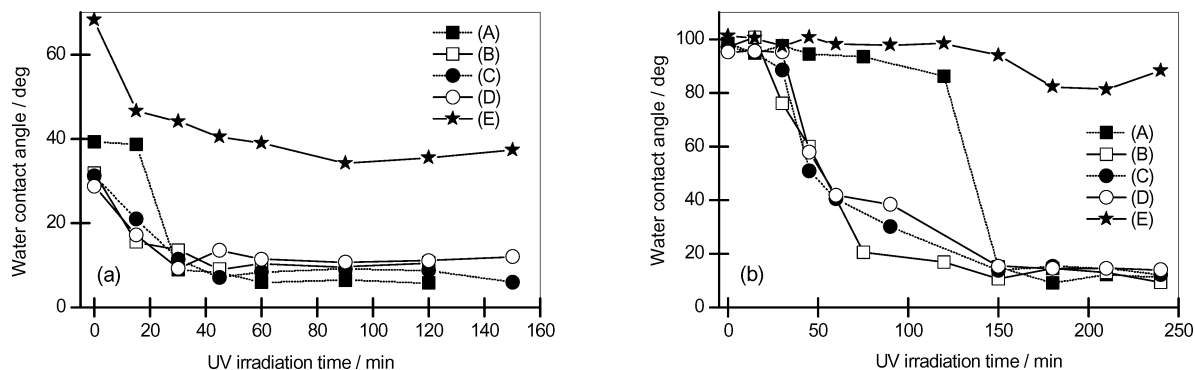
Fig. 5 Evolution of the water contact angle as a function of UVA irradiation time on aged (a) and methyl-stearate contaminated (b) thin films: (A) TiO_2 heat-treated at 100 °C, (B) TiO_2 at 500 °C, (C) TiO_2–ZrO_2 at 100 °C, (D) TiO_2–ZrO_2 at 500 °C, and (E) Pilkington Activ™ glass.

hydrophilicity of the sol–gel films, but on photocatalytic activity it did not have a significant positive effect. Zirconia at a content of 10% with respect to titania was found to be homogeneously distributed along the film thickness, presumably in its amorphous modification. The films treated at low temperatures were found to have superior efficiency towards degradation of Plasmocorinth B aqueous solution since sufficient crystallinity was developed already during the sol formation. The photodegradation of the methyl stearate solid layer was fast also when deposited on the films treated at high temperatures, proving the self-cleaning ability of both kinds of films.

Acknowledgements

Notes and references

1 M. Kaneko, I. Okura, *Photocatalysis: Science and Technology*, Springer, Berlin, 2002; I. P. Parkin and R. G. Palgrave, *J. Mater. Chem.*, 2004, **15**, 1689–1695; O. Carp, C. L. Huisman and A. Reller, *Prog. Solid State Chem.*, 2004, **32**, 33–177; U. Diebold, *Surf. Sci. Rep.*, 2003, **48**, 53–229; A. Mills and S.-K. Lee, *J. Photochem. Photobiol. A: Chem.*, 2002, **152**, 233–247; J. Zhao and X. Yang, *Building Environ.*, 2003, **38**, 645–654; A. Fujishima, T. N. Rao and D. A. Tryk, *J. Photochem. Photobiol. C: Photochem. Rev.*, 2000, **1**, 1–21.
2 E. L. Crepaldi, G. J. de A. A. Soler-Illia, D. D. Grosso, F. Cagnol, F. Ribot and C. Sanchez, *J. Am. Chem. Soc.*, 2003, **125**, 9770–9786; P. Bouras, E. Stathatos and P. Lianos, *Appl. Catal. B: Environ.*, 2007, **73**, 51–59; U. L. Štangar, U. Černigoj, P. Trebše, K. Maver and S. Gross, *Monatsh. Chem.*, 2006, **137**, 647–655.
3 Y. J. Yun, J. S. Chung, S. Kim, S. H. Hahn and E. J. Kim, *Mater. Lett.*, 2004, **58**, 3703–3706; Y. Hu and C. Yuan, *J. Cryst. Growth*, 2005, **274**, 563–568; U. L. Štangar, U. Černigoj, K. Maver, P. Trebše, S. Gross, in *New Research on Thin Solid Films*, ed. M. G. Benjamin, Nova Science Publishers, New York, 2007, ch. 3, pp. 107–132.
4 M. Addamo, M. Bellardita, A. Di Paola and L. Palmisano, *Chem. Commun.*, 2006, 4943–4945.
5 P. Novotná, J. Zita, J. Krýsa, V. Kalousek and J. Rathouský, *Appl. Catal. B: Environ.*, 2007, **79**, 179–185.
6 D. G. Shchukin, J. H. Schattka, M. Antonietti and R. A. Caruso, *J. Phys. Chem. B*, 2003, **107**, 952–957.
7 M. D. Hernández-Alonso, I. Tejedor-Tejedor, J. M. Coronado, J. Soria and M. A. Anderson, *Thin Solid Films*, 2006, **502**, 125–131.
8 X. Fu, L. A. Clark, Q. Yang and M. A. Anderson, *Environ. Sci. Technol.*, 1996, **30**, 647–653.
9 J. H. Schattka, D. G. Shchukin, J. Jia, M. Antonietti and R. A. Caruso, *Chem. Mater.*, 2002, **14**, 5103–5108.
10 B. Neppolian, Q. Wang, H. Yamashita and H. Choi, *Appl. Catal. A: General*, 2007, **333**, 264–271.
11 N. Smirnova, A. Eremenko, V. Gayvoronskij, I. Petrik, Y. Gnatyuk, G. Krylova, A. Korchev and A. Chuiko, *J. Sol–Gel Sci. Technol.*, 2004, **32**, 357–362.
12 W. Zhou, K. Liu, H. Fu, K. Pan, L. Zhang, L. Wang and C. Sun, *Nanotechnol.*, 2008, **19**, 035610 (7 pp.).
13 J. F. Moulder, W. F. Stickle, P. E. Sobol, K. D. Bomben, in *Handbook of X-Ray Photoelectron Spectroscopy*, ed. J. Chastain, Perkin Elmer Corp.: Eden Prairie, MN, 1992; *X-ray Photoelectron Spectroscopy Database 20* [Version 3.0], National Institute of Standards and Technology, Gaithersburg, MD, http://srdata.nist.gov/XPS.
14 U. Černigoj, U. L. Štangar, P. Trebše, U. O. Krašovec and S. Gross, *Thin Solid Films*, 2006, **495**, 327–332.
15 S. R. Patil, U. L. Štangar, S. Gross and U. Schubert, *J. Adv. Oxid. Technol.*, 2008, **11**, 327–337.
16 C. Guillard, D. Debayle, A. Gagnaire, H. Jaffrezic and J. M. Herrmann, *Mater. Res. Bull.*, 2004, **39**, 1445–1458; I. N. Martyanov and K. J. Klabunde, *J. Catal.*, 2004, **225**, 408–416.
17 T. Choudhury, S. O. Saied, J. L. Sullivan and A. M. Abbot, *J. Phys.: Appl. Phys.*, 1989, **22**, 1185–1195.
18 L. Armelao, D. Bleiner, V. Di Noto, S. Gross, C. Sada, U. Schubert, E. Tondello, H. Vonmont and A. Zattin, *Appl. Surf. Sci.*, 2005, **249**, 277–294; L. Armelao, H. Bertagnolli, S. Gross, V. Krishnan, U. L. Štangar, K. Müller, B. Orel, G. Srinivasan, E. Tondello and A. Zattin, *J. Mater. Chem.*, 2005, **15**, 1954–1965; L. Armelao, C. Eisenmenger-Sittner, M. Groenewolt, S. Gross, C. Sada, U. Schubert, E. Tondello and A. Zattin, *J. Mater. Chem.*, 2005, **15**, 1838–1848.
19 R. Cerc Korošec, P. Bukovec, B. Pihlar and J. Padežnik Gomilšek, *Thermochim. Acta*, 2003, **402**, 57–67; R. Cerc Korošec and P. Bukovec, *Acta Chim. Slov.*, 2006, **53**, 136–147.
20 B. M. Reddy and A. Khan, *Catal. Rev. Sci. Eng.*, 2005, **47**, 257–296.
21 U. Černigoj, U. L. Štangar and P. Trebše, *J. Photochem. Photobiol. A: Chem.*, 2007, **188**, 169–176; L. Armelao, D. Barreca, G. Bottaro, A. Gasparotto, C. Maccato, C. Maragno, E. Tondello, U. L. Štangar, M. Bergant and D. Mahne, *Nanotechnol.*, 2007, **18**, 375709–375716.